Journal of Civil Structural Health Monitoring (2024) 14:3–14
https://doi.org/10.1007/s13349-022-00605-0

ORIGINAL PAPER

Monitoring and identification of wire breaks in prestressed concrete cylinder pipe based on distributed fiber optic acoustic sensing

Yanlong Li[1] · Kaiyu Sun[1] · Zheng Si[1] · Fang Chen[2] · Lei Tao[2] · Kangping Li[1] · Heng Zhou[3]

Received: 22 March 2022 / Revised: 30 June 2022 / Accepted: 1 July 2022 / Published online: 9 August 2022
© Springer-Verlag GmbH Germany, part of Springer Nature 2022

Abstract
Prestressed concrete cylinder pipes (PCCPs) have become increasingly competitive in pipeline transportation due to several advantages such as high pressure-bearing capacity and good durability. Unfortunately, corrosion and deterioration would cause certain PCCPs to fail after an amount of time in service. To assess the condition of pipelines and to eliminate catastrophic consequences, long-term monitoring is necessary. In this study, a novel method based on distributed acoustic sensing (DAS) technology, was presented to monitor and identify wire breaks in PCCP under different conditions such as corrosion and hydrogen embrittlement. The findings revealed that DAS has a recognition accuracy for vibration, particularly wire breaks, and captures wire breaks and noise at multiple locations in a variety of environments quickly and efficiently. Wire break signals in different environments have both similarities and differences. From the time-domain perspectives of amplitude, duration, short-time zero-crossing rate, and short-time energy, the wire's break and noise could be effectively discriminated. The wires will break without warning after reaching the ultimate bearing capacity, which is related to the internal water pressure. The nature of its break is the release of internal energy, independent of the factors that make it fracture, such as substandard wire quality and erosion.

Keywords Prestressed concrete cylinder pipes (PCCPs) · Distributed acoustic sensing (DAS) · Wire breaks · Monitor and identification

1 Introduction

With the development of the economy and the improvement of residents' living standards, the transmission of water resources and the discharge of urban sewage are of particular importance. Since its introduction in the 1940s, prestressed cylinder concrete pipes (PCCPs) are widely used and developed in the world due to many advantages including water transmission capacity and durability in pipelines, such as the Central Arizona Project in California, the Great Man-made River Project in Libya, Africa [1] and the South-to-North Water Diversion Project in China [2]. The American Concrete Pressure Piping Association (ACPPA) reports that 90% of water utilities in the United States use PCCPs in water supply projects [3, 4].

Corrosion is a significant problem on bridges, dams, tunnels, pipelines, and other buildings. Globally, the associated cost is estimated at billions of dollars per year [5]. The corrosion of prestressed wires by corrosive ions such as chloride ions in the soil is the most common way to cause PCCP failure [6, 7]. The generation and increase of broken wires is an important reason for the damage of PCCP and an extremely serious safety problem during the operation of the pipelines. Its impact on the structural performance of pipelines and reinforcement of PCCP after wire break is the current research trend, and numerous studies have been conducted [8–10]. Zhai et al. [11] proposed a theoretical model for calculating the stress distribution of steel wires by assuming a linear distributed pattern of bond stress, and also developed a three-dimensional finite element model of PCCP to calculate the effect of the number of broken wires on the bearing capacity of PCCP. The results indicate that

✉ Yanlong Li
liyanlong@xaut.edu.cn

1 State Key Laboratory of Eco-Hydraulics in Northwest Arid Region, Xi'an University of Technology, Xi'an 710048, China

2 Hanjiang-to-Weihe River Valley Water Diversion Project Construction Co., Ltd., Xi'an 710010, China

3 Power China Northwest Engineering Corporation Limited, Xi'an 710065, Shaanxi, China

the bearing capacity of PCCP decreases with the increase of wire breakage ratio, but the decreasing trend slows down. The further development of the broken wires will make the concrete core crack under external loads and eventually fail. According to the damage of many conveyance projects, PCCP bursts are sudden, catastrophic, and unpredictable. After the pipeline explosion, it will not only cause significant losses of water resources but major losses to the public and the economy [12]. Therefore, it is essential to guarantee the normal operation of pipelines and to conduct long-term safety monitoring of pipelines.

The industry has been focusing on the monitoring of broken wires in PCCP pipelines, and a lot of research has been conducted. To ensure the adequate safety and reliability of PCCPs in service, a series of non-destructive testing techniques have been applied. Wardany [13], Rizzo [14], and Liu [15] summarized the inspection and assessment methods for PCCP pipelines and analyzed the advantages and disadvantages. Traditional inspection methods include Visual Inspection, Visual and Hammer Sounding Inspection, and Sonar et al., however, these methods have different degrees of limitations and are difficult to apply to long-distance pipeline monitoring [16, 17]. Subsequently, the Sonic/Ultrasonic Method [18, 19], acoustic emission technique [20–22], resonant acoustic spectroscopy [23], the orthogonal electromagnetic principle [24, 25], and distributed fiber optic sensors [26–29] have been widely used in the field of non-destructive monitoring of PCCPs. Elfergani et al. [21] conducted a PCCP test block simulation under laboratory conditions and monitored the entire process of electrochemical corrosion wire breaks for 14 days using acoustic emission technology, proving that acoustic emission can identify wire breaks as well as early corrosion cracking of the concrete, but it is difficult to apply the safety monitoring of long-distance transmission pipelines. Xie et al. [25] implemented a broken wires detection of PCCP based on orthogonal electromagnetic principle and established an orthogonal electromagnetic wire breaks detection system. However, the method has some limitations: change of conductivity in wires and steel cylinders cause irregular background noise, making it difficult to accurately identify the occurrence of wire breaks and requiring experienced personnel to reduce the false alarm phenomenon. Wei et al. [30] undertook a 6-month investigation for PCCP corrosion utilizing Low-coherent fiber-optic sensors (LCFS) technology. The findings indicated that LCFS is a helpful method for long-term monitoring of structures from early localized deterioration to eventual failure under corrosive action, but the measurement results are susceptible to external perturbations. Hu et al. [12] carried out a PCCP prototype bearing capacity test with a different number of broken wires. After removing the mortar coating from the local location of the PCCP, the wire was broken by manual cutting, and the effect of the number of broken wires on the bearing performance of the PCCP is measured by placing stress–strain sensors on the wire surface, the outer concrete surface and the mortar coating. The results showed that: when the percentage of broken wires reaches 10%, the bearing capacity of the pipelines will rapidly deteriorate, the experimental findings were in good agreement with the calculated results of numerical simulation conducted on a PCCP prototype test and numerical simulation.

As a practical and promising monitoring method, distributed fiber optic sensing technology has many advantages such as small size, lightweight, corrosion resistance, anti-electromagnetic interference, etc. It could be embedded inside the structure or attached to the surface, especially suitable for long-distance detection, and has a high degree of fit with pipelines safety monitoring. Huang et al. [31] proposed a safety monitoring scheme for building glass windows based on distributed fiber optic sensing, using the Wigner dual-spectrum analysis method to perform time–frequency analysis of vibration signals and extract feature vectors, believing that DAS could be an effective monitoring technique for the accurate identification of different types of interference events with an average recognition rate of 93.3%. Cao et al. [32] applied distributed acoustic sensing fiber (DASF) based on phase-sensitive optical time-domain reflection (Φ-OTDR) to underwater target detection in a lake with an average depth of 9 m, demonstrating that the data received by the underwater distributed optical fiber system can better reconstruct the acoustic source information in shallow water, and the feasibility of DASF sensing underwater acoustic signals in shallow water is verified, which indicates that DAS technology could be applied to PCCP pipeline safety monitoring. Muggleton et al. [33] buried the distributed optical fiber in the ground and monitored noise at the leakage point to determine the operating condition of the oil and gas pipelines. They concluded that the distributed optical fiber could be used for long-term effective pipe leakage monitoring, and the closer the optical fiber is to the vibration location, the better the monitoring effect, demonstrating that distributed optical fiber could be applied to long-term monitoring of the safety performance of PCCP pipelines. In conclusion, distributed optical fiber has strong environmental adaptability and durability, and has a broad development prospect in the field of engineering safety monitoring. Therefore, it is feasible to apply distributed fiber optic sensing technology to the safety monitoring of PCCP pipelines. In this paper, the fracture of prestressed wires in an embedded-cylinder pipe (ECP) was monitored and identified utilizing distributed fiber optic sensing (DAS) technology in different situations. Optical fiber was deployed on the inner and outer walls of the PCCP, and DAS was applied to capture and analyze the wire breaks and noise, and to perform time-domain analysis to obtain the general characteristic criteria of wire break signals, which provides a certain basis for PCCP wire breaks monitoring in practical projects.

2 PCCP specimen and DAS system

2.1 Prestressed concrete cylinder pipe

Prestressed concrete cylinder pipe, as a typical composite pipe, is mainly composed of the concrete core, steel cylinder, high-strength prestressed wires, and mortar coating. There are two types of PCCPs [16, 34]: the lined cylinder pipe (LCP) and the embedded-cylinder pipe (ECP, shown in Fig. 1). The difference between them is mainly reflected in structure and pipe diameter size, the latter has a greater bearing capacity and higher water transmission capacity. Therefore, ECP possesses great application value and development potential in long-distance and high-flow water transmission projects. PCCP gives full play to the advantages of different materials such as concrete pressure resistance, steel cylinder seepage resistance, and wire tensile resistance, so it has a long design service life (generally more than 50 years). The specimen in this test was an ECP designed in accordance with the Standard for the Design of Prestressed Concrete Cylinder Pipe (ANSI/AWWA C304-2014) [16]. The geometry and material parameters of PCCP are shown in Table 1.

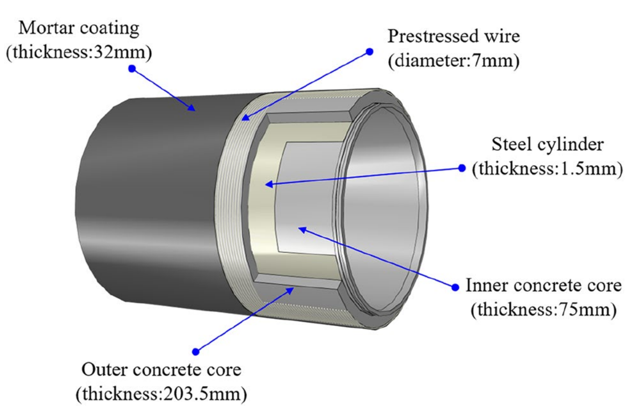

Fig. 1 Structure diagram of PCCP

2.2 Distributed fiber acoustic sensing

Based on Φ-OTDR for monitoring, DAS is a sensing technology that utilizes the coherent decay effect of fiber backscattering Rayleigh Backscattering (RBS) to achieve long-distance, distributed, real-time quantitative monitoring of the new sensing technology. It has two significant advantages: fast response (millisecond or even sub-millisecond) and high detection sensitivity (nano-strain).

The MS-DAS system is a world-leading distributed acoustic sensing device, which continuously records the acoustic signal transmission and spatial distribution of the acoustic field along with the long-distance fiber. The system is capable to detect strains as small as sub-nano-strain, and the response band covers from infrasound to ultrasound, which was applied to the distributed measurement of seismic waves, micro-vibrations, micro-strains, etc. It has great potential for application in the fields, such as resource exploration and secure collection [35], pipeline safety [33, 36], seismic monitoring [37], perimeter safety [38], and structural health of projects [39, 40]. At present, the product has been developed to the second generation MS-DAS2000II, which has higher sensitivity and better signal-to-noise ratio, and the waveform fidelity is greater than 95% and is also the monitoring equipment used in this test, as shown in Fig. 2.

The DAS can be thought of as a moving interferometric acoustic sensor that detects external signals through a sensing fiber, and its operating principle is shown in Fig. 3. External sound or vibration will influence the phase of the interferometric light, and quantitative measurement of external physical quantities may be accomplished by extracting the interferometric signal during different moments at that location and demodulating it. The biggest feature is that it can perform continuous distributed measurements, which is equivalent to an array of infinite hydrophones. The light source signal is generated by a narrow linewidth laser with a wavelength of 1550 nm and a linewidth of 100 Hz. After

Table 1 Geometry and material parameters of PCCP

Geometric parameters	Value (mm)	Mechanical parameters	Value (MPa)
Length of pipe	5000	Internal working pressure	0.8
Inner diameter	3400	The design value of internal pressure	1.12
Inner core thickness	75	Standard compressive strength	55
Steel cylinder thickness	1.5	Strength of steel cylinder	215
Outer core thickness	203.5	Strength of prestressing wire	1570
Diameter of wire	7	Initial prestressing of wire	1177.5
Spacing of wire	16.5	Standard compressive strength of mortar coating	45
Coating thickness	32		

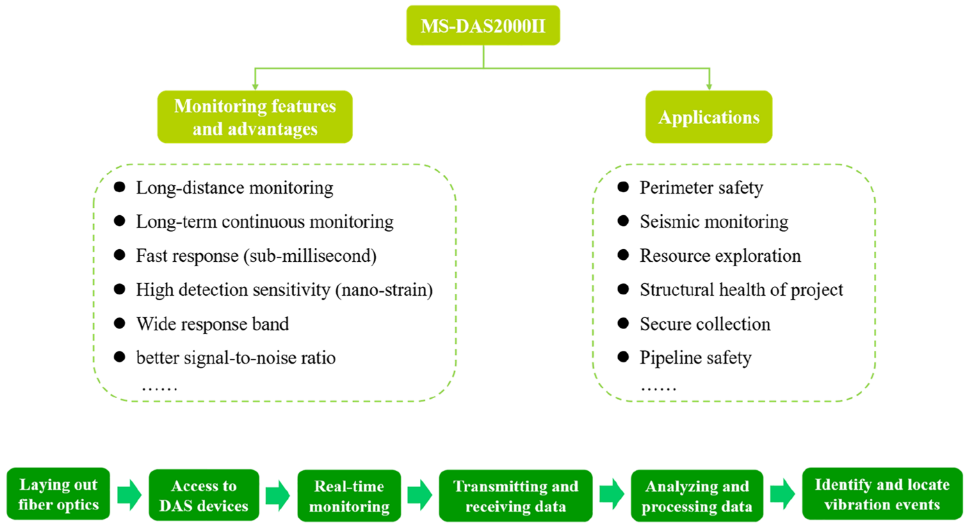

Fig. 2 MS-DAS2000II features and applications

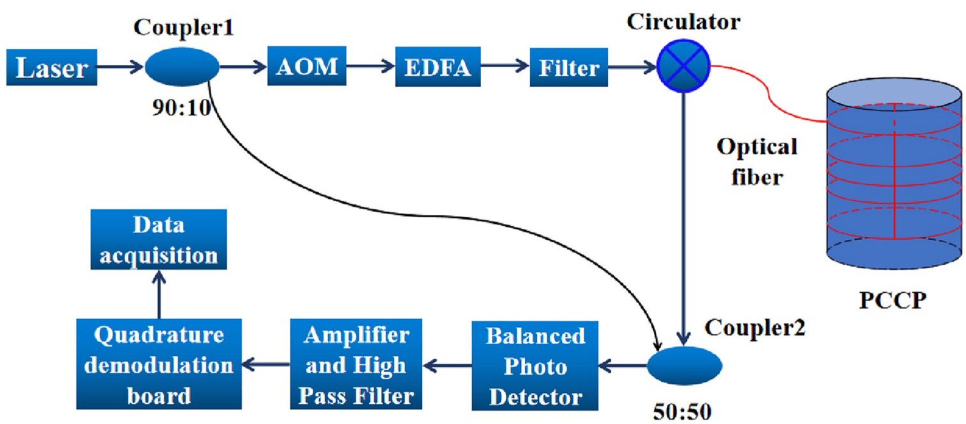

Fig. 3 Working principle diagram of distributed optical fiber acoustic sensing. AOM: acoustic optic modulator. EDFA: erbium doped fiber amplifier

passing through the optical coupler 1, the optical signal is divided into two parts, 90% of which is used as the detection optical signal and 10% of which is the reference optical signal. The detection light is modulated into optical pulses by the acoustic-optic modulator (AOM), amplified by the erbium-doped fiber amplifier (EDFA), and then sent through the optical fiber, where Rayleigh scattering occurs with the fiber medium, resulting in Rayleigh scattered light. When the surrounding stress and vibration cause the Rayleigh scattered light phase change, the distributed fiber optic vibration sensing system will detect the intrusion signal according to the coherent interference light wave change of Rayleigh scattered light. By coherent beat frequency, the light intensity (I) obtained by the photodetector can be expressed as [31]:

$$I \propto 2E_{LO}E_z\cos\left(\Delta ft + \varphi_z'\right) \quad (1)$$

where E_{LO} and E_z are the optical field intensities of the local oscillation light and Z-point Rayleigh scattering signal, respectively, Δf denotes the optical frequency difference between the two lights, and φ_z' denotes the phase difference between the two lights. Using the in-phase quadrature (IQ) demodulation algorithm, the phase difference φ_z' can be calculated. The returned fiber optic signal is converted into a light intensity signal through the circulator, and the backscattered light signal and the reference light signal are coupled in a 50:50 ratio through coupler 2. Finally, the balanced photodetector (BPD) converts the light signal into an electrical signal, and the data acquisition card performs signal acquisition to realize the analysis and processing of the intrusion vibration signal by the distributed fiber optic sensing system. The DAS system monitoring parameters are shown in Table 2, and monitoring distance and accuracy are still being improved.

3 Experimental study

3.1 Model selection and layout of optical fiber

The fiber type selected in this experiment is NZS-DSS-C09, and its attachment substrate is a fabric strip made of the

Table 2 DAS system monitoring parameters

Parameters	Value
Monitoring distance	≤20 km
Sampling frequency	≤30 kHz
Refractive index	1.468
Spatial resolution	≥1 m

carbon fiber cloth, glass fiber cloth, and aramid cloth, which with a width of 3 cm are composite materials made of fibers with high strength, as well as ultra-light, high-temperature and high-pressure resistance. As an attachment matrix, it has a certain protective effect on the fiber, and increases the contact area between the fiber and the structure, leading to closer integration of both, making data collecting and monitoring easier and maintaining the correctness and reliability of monitoring data. Its construction is illustrated in Fig. 4.

As shown in Fig. 5, the optical fiber was installed at 1, 2.5, and 4 m using spiral winding on the inner and outer walls of PCCP. The total length of the fiber optic is roughly more than 80 m, of which, the inner and outer walls are about 40 m, respectively. In the process of laying, use glue and epoxy resin to fix the optical fiber to ensure good contact between it and PCCP. A detailed diagram of the fiber optic placement on the PCCP is depicted in Fig. 6.

3.2 Experiment

After laying out the optic fiber, we conducted three groups of PCCP broken wire tests in turn. The MS-DAS2000 III was used to monitor the wire breaks under different environments and the noise generated during the tests. Based on the comprehensive consideration of measurement accuracy and spatial resolution, the sampling frequency was determined to be 1 kHz and the spatial resolution was 2 m.

During the operation of the PCCP pipelines, the different factors that cause the fracture of the prestressed wires can be roughly divided into two categories: wire breaks due to unqualified production processes and long-term erosion of corrosive ions in the soil makes wire breaks. The former is more probable to occur in the early stages of PCCP pipeline operation, and the latter increases significantly with the duration of PCCP pipeline service. In this test, the electrochemical accelerated corrosion method was used to simulate

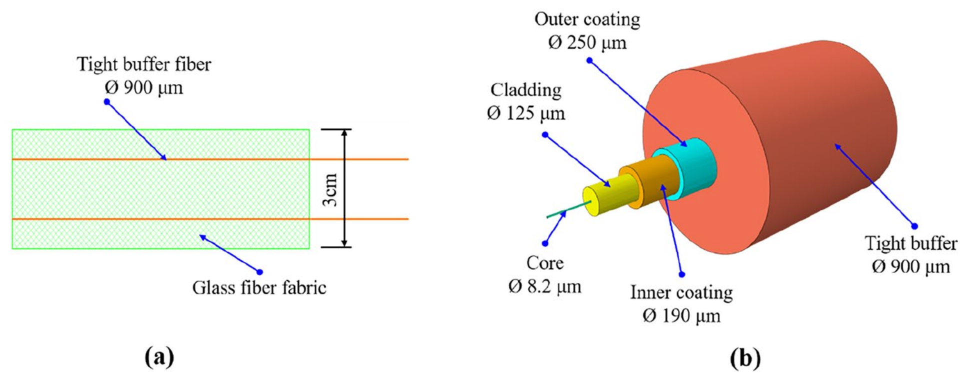

Fig. 4 **a** 900-μm-diameter tight buffer fiber with glass fiber fabric. **b** Illustration of the cross-section of an optical fiber

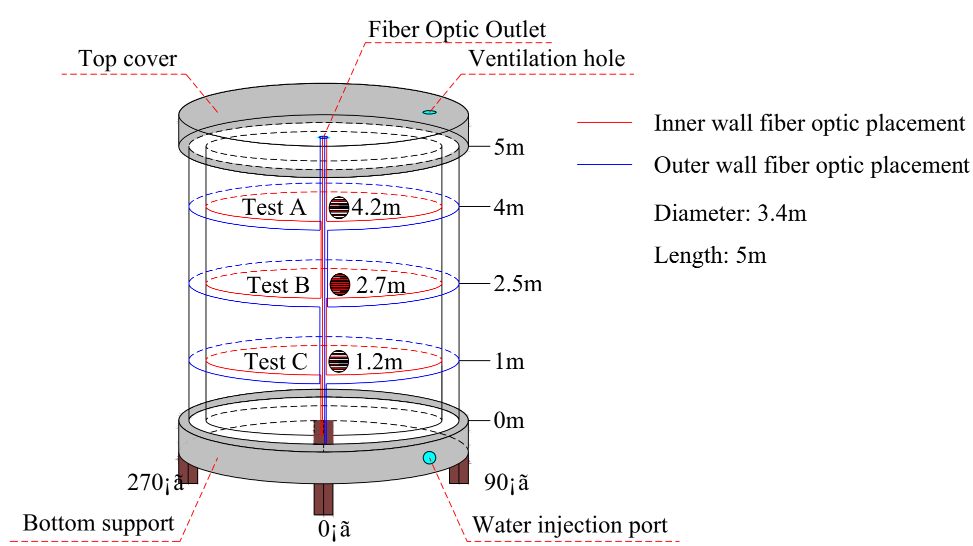

Fig. 5 The layout of the optical fiber on the inner and outer walls of the pipe and the distribution of broken wires tests

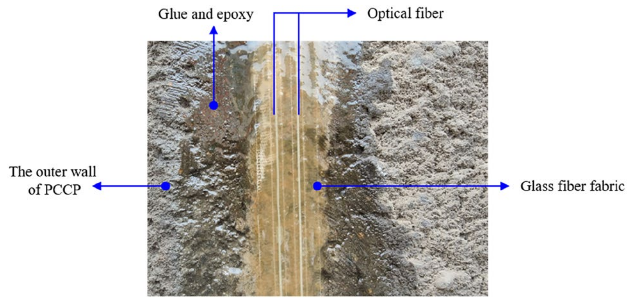

Fig. 6 A detailed diagram of the fiber optic placement on the PCCP

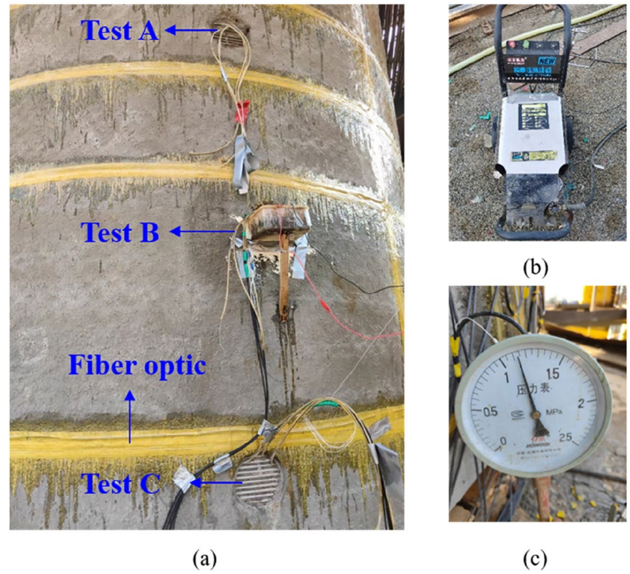

Fig. 7 **a** Overall picture of the PCCP wire breaking test site; **b** Equipment to control the water pressure in the PCCP; **c** Internal pressure monitoring gauge of the PCCP

the corrosion of broken wires, and artificial cutting simulated the broken wires of hydrogen embrittlement. According to the different types of wire breaks and internal water pressure, the wire breaks test is divided into three groups: cutting wire breaks without internal pressure (Test A), corrosive wire breaks under normal working internal pressure (Test B), and cutting wire breaks under normal working internal pressure (Test C). The overall picture of the PCCP wire breaking test site and the equipment to control the water pressure in the PCCP are shown in Fig. 7.

It can be seen in Fig. 5, test A was conducted at a height of 4.2 m from the bottom, under the condition of without internal pressure, and three adjacent wires (A1, A2, A3) were cut in sequence. Subsequently, the internal water pressure was applied in step-by-step pressurization, and the pressure was stabilized for 5 min for each 0.1 MPa increase. And the wires in test B were electrochemically accelerated and corroded with a 5% NaCl solution by an impressed current. The steel wire was used as the anode, connected to the positive side of the power supply, and a copper sheet was placed at the cathode and connected to the negative side of the power supply, producing a closed circuit for the corrosion test. A regulated power source controls and regulates the corrosion current, which is 10 mA/cm^2. Tests B and C were conducted at a height of 2.7 and 1.2 m from the bottom, respectively, when the internal pressure reached normal operating pressure (0.8 MPa). The cutting wire breaks test and the corrosion wire break test are shown in Fig. 8. During the whole experience, the MS-DAS2000III was employed to continuously monitor the occurrence of wire breaks and noise at the test site.

4 Results and discussion

4.1 Time domain distribution of broken wire signals

Figure 9 shows the time-domain diagrams of fiber at nine separate locations during the break of the B2 wire. As seen in Fig. 9, DAS could monitor and collect wire breaks in different environments instantly. When there is no vibration around the optic fiber, the monitoring signal is relatively stable and fluctuates slightly around 0, which is the system noise. From Fig. 9a, (i), it is clear that the signals at both ends of the fiber are promiscuous, which generated a large amount of noise, making it difficult to identify broken wires effectively. Correspondingly, Fig. 9b-h show that the fiber installed on both the inner and outer walls of the PCCP, and provides accurate and efficient capture of the occurrence of wire breaks. The maximum amplitude of the broken wire signal fluctuates around 3 and the duration is roughly 2 s, which is a typical non-stationary signal. The occurrence of wire breaks is unpredictable, sudden, and unpredictable, making it impossible to predict.

4.2 Pre-processing of the original signal

Due to the interference of noise, it is inevitable to make the effective signal mixed with a large number of invalid signals, and if the monitoring data is analyzed directly, it not only requires a lot of calculations but also is difficult to achieve excellent recognition results. Consequently, it is necessary to pre-process the original data and extract features accordingly. Considering that the signal of a broken wire at different locations of the fiber has little difference, we selected three groups of typical signals from wire break tests and environmental noise to perform pre-processing and comparative analysis, respectively.

Since the PCCP pipelines are in a complex environment and the amount of monitoring data is enormous, the

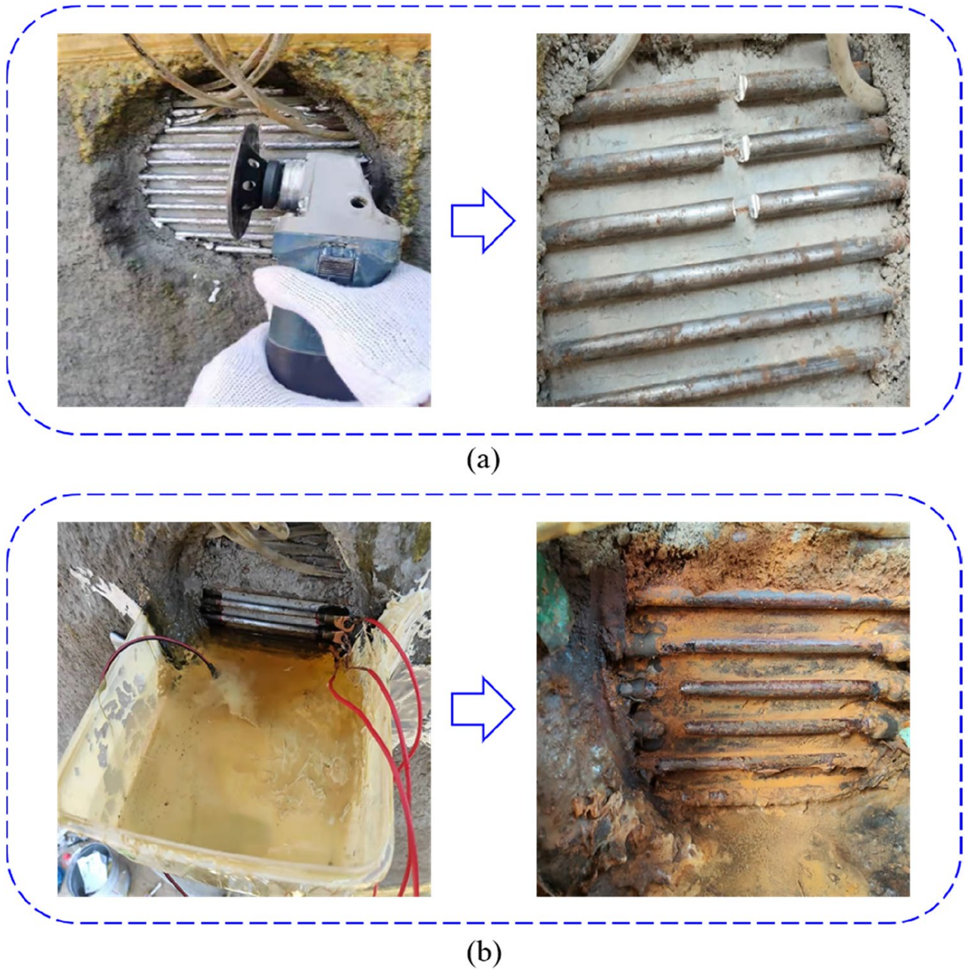

Fig. 8 **a** Artificial cutting of wires. **b** Electrochemical corrosion of wires

common Daubechies (db) wavelet is applied to denoise the original signal. The db wavelet has the characteristics of better regularity, smoothness, and tight support, and one of the Haar (db1) wavelets has the advantages of simple calculation, and high efficiency, which enables to satisfy the requirements of real-time monitoring, so the Haar wavelet is employed to denoise the original signal. Based on the comprehensive consideration of accuracy and computation, the level of decomposition layers of wavelet denoising is chosen as 4. The denoising methodology is the Minimax method, which is designed to find the local optimal solution instead of the global optimal solution. Considering that the wire breaks occur at the local location of PCCP and have a large difference with the environmental noise, the algorithm has a high degree of fit with the wire break monitoring. The soft threshold function is adopted to ensure better continuity of the signal after de-noising.

Figure 10 presents the time-domain diagrams of the original signal and the de-noised signal for the three groups of broken wires and noise. The broken wire signals differ greatly from the noise signal in terms of amplitude magnitude and distribution properties, as shown in Fig. 10. While filtering out most of the ambient and system noise, the de-noise signal efficiently retains the properties of the broken wire signals. The difference in the amplitude of the three groups of broken wire signals is not significant, while the duration has a large difference. The duration of test A was 0.9 s, and the duration of tests B and C were basically the same, 1.8 and 1.7 s, respectively, roughly twice as long as test A. During the operation of the pipeline, the common vibration events and environmental noise generated in and around itself are low-frequency signals, thus we pay greater attention to low-frequency vibration events during the test, such as wire breaks, and set a lower sample frequency and filter the high-frequency signal throughout the monitoring. Meanwhile, because the wire in the process of corrosion is essentially static, and the corrosion reaction on the PCCP is extremely weak, it's difficult to lay the fiber on the tube's wall to produce vibration, and the influence on the time domain waveform of the broken wire is minimal.

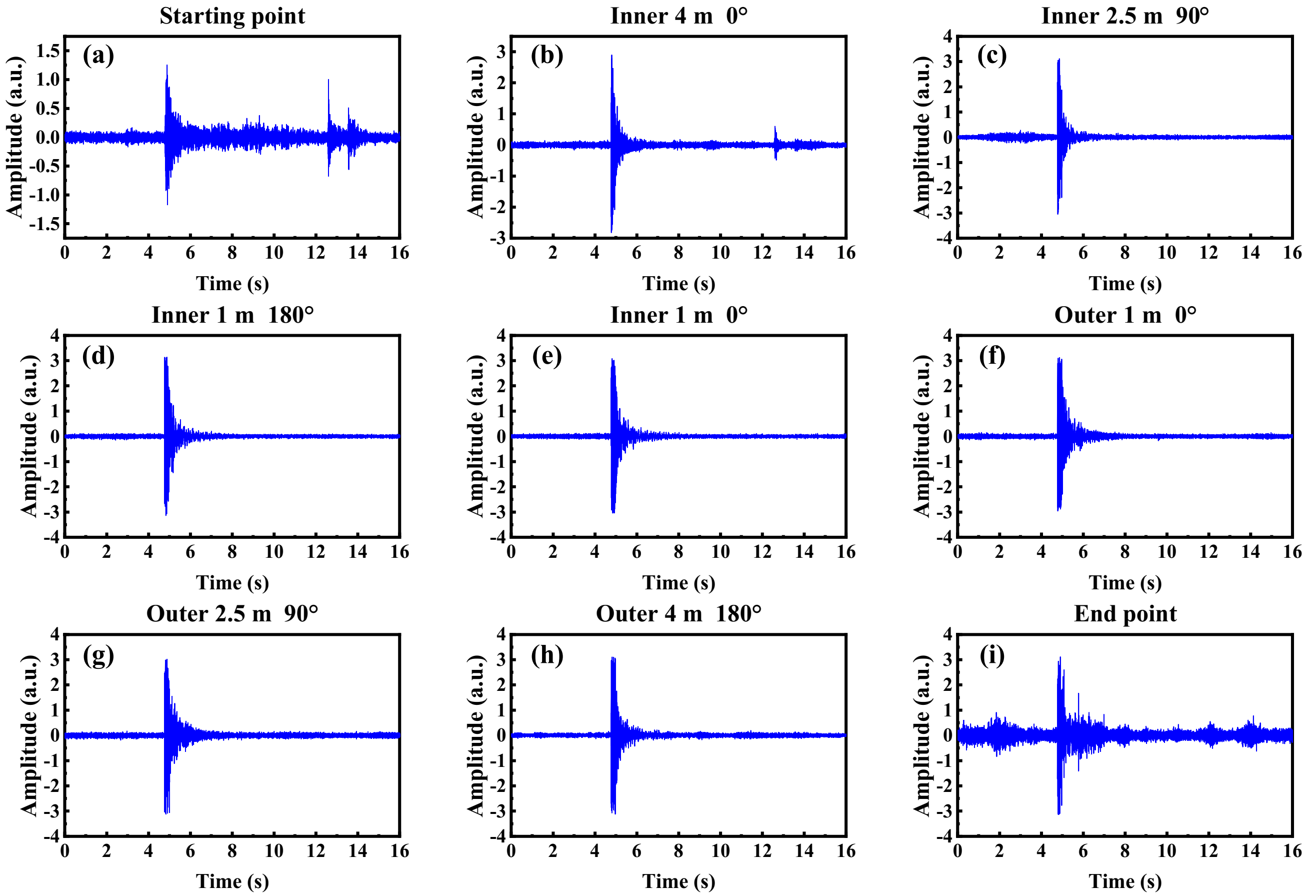

Fig. 9 The time-domain waveforms at different positions when the B2 wire was broken

4.3 Time-domain analysis

As a classic method to extract signal features, time-domain analysis is commonly used to analyze the processing of signals. It is concerned with the time-domain characteristics of the signals, such as amplitude, duration and repetition period, etc. Therefore, it is especially suitable for processing non-stationary signals. To guarantee the data integrity and accuracy, we divided the signal into frames with a frame length of 200 ms, partial overlap of adjacent frames, and a frameshift of 80 ms to ensure a smooth transition of the signal frames, and calculated the short-time zero-crossing rate and short-time energy of the signals for further analysis and comparison of the broken wires and noise.

Figure 11a indicates the short-time zero-crossing rate of the original broken wire signals and the noise signals. When there is no vibration, the zero-crossing rate of system noise is stable at approximately 140/frame (700/s). And if there is an external vibration intrudes, the signal fluctuation amplitude will increase, and consequently, the zero-crossing rate will decrease. When the signals were de-noised and reconstructed, the degree of fluctuation of the system noise was significantly reduced and there was a significant difference in the over-zero rate of the broken wire signal and the environmental noise. As shown in Fig. 11b, the peak short-time zero-crossing rates of the three groups of broken wire tests are approximately the same, roughly 400–500/s, while the over-zero rate of noise is lower, with a maximum of only 140/s, which is different with broken wire signals.

The short-time over-zero rates of the three groups of wire break tests exhibit a high degree of resemblance and are distinct from the noise, enabling the wire break and noise to be distinguished. The broken wire tests B and C were operated under normal working internal pressure, while test A was performed without internal pressure. The former wire bears more stress than the latter, therefore the break occurs when the peak over zero rates is also larger, indicating that the internal water pressure has a stronger influence on the wire break vibration signal. Under the same conditions of internal water pressure, although the factors causing wire breaks in tests B and C were not different, the over-zero rate trend of both was very similar, which indicated that the wire break signals were not related to the external factors causing wire breaks.

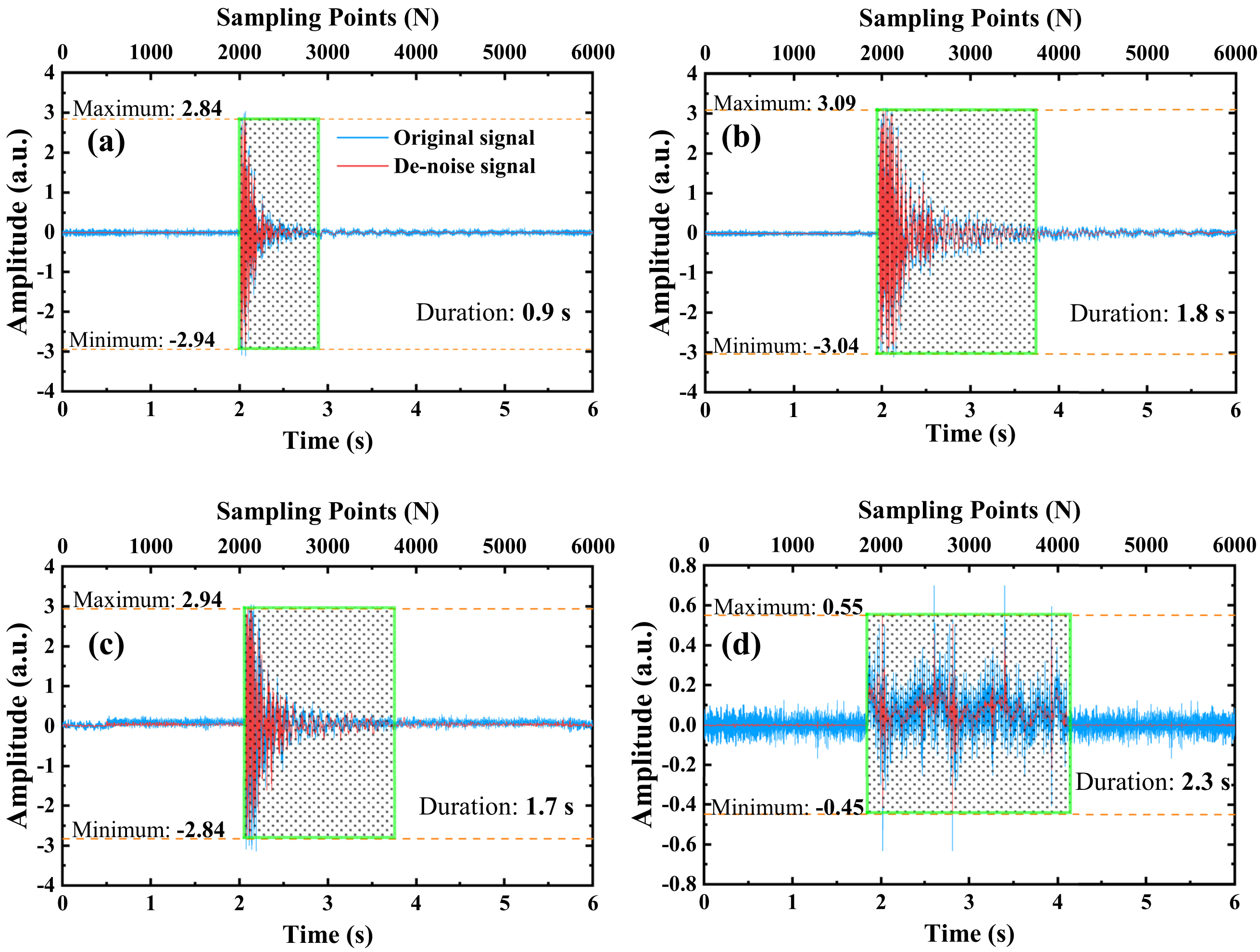

Fig. 10 The time-domain diagram of the original signal and the de-noise signal of the three groups of broken wires and noise. **a** Cutting and breaking wires without pressure internal water, Test A. **b** Corrosion broken wires under normal working internal water pressure, Test B. **c** Cutting and breaking wires under normal working internal water pressure, Test C. **d** Noise under normal working internal water pressure

Considering that the wire break without any premonition and its energy when breaking is suddenly released in a short period, the occurrence of wire breaks can be identified and captured from short-time energy. Figure 12 shows the short-time energy diagram of the de-noise signal of three groups of broken wire signals and noise signals. The noise's energy is significantly lower than the energy released when the wire breaks, and it's nearly non-existent. From the standpoint of short-term energy, it is easier to monitor and catch wire breaks throughout the monitoring process. Tests B and C had more total energy and were not substantially different, with 56.22 and 65.03, respectively, however, test A had just 28.94, which was about half of test B. After peaking, the attenuation time of the latter was also shorter than the former. The reason is that when the PCCP is full, the wire fracture energy released by the tube is temporarily "stored" in the water, causing the speed of dissipation to be slower and the vibration time to be longer; when the tube is empty, the energy quickly dissipates in the air, causing the vibration time to be shorter, and the total energy smaller.

4.4 Discussion

In conclusion, the generation of broken wires could be accurately and efficiently determined from the time-domain perspectives of signal amplitude, short-time zero-crossing rate, and short-time energy. While the wires of Test B and Test C break in different ways, the time-domain characteristics of the two groups are extremely similar. The reason is that the nature of wire breaks is the release of internal energy, independent of the external factors causing its fractures, such as corrosion and hydrogen embrittlement. Both wires of Test A and Test C were cut, but the former was smaller than the latter in terms of energy, duration, and many other aspects.

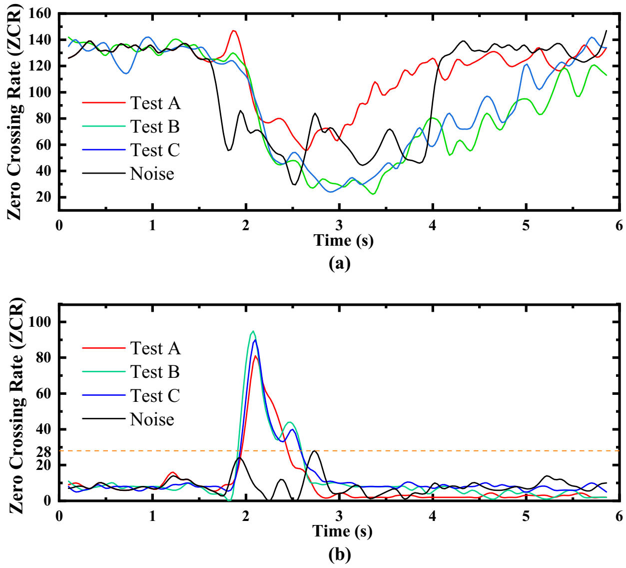

Fig. 11 Short-time zero-crossing rate distribution diagram of three groups of broken wire tests. **a** Original signals. **b** De-noise signals

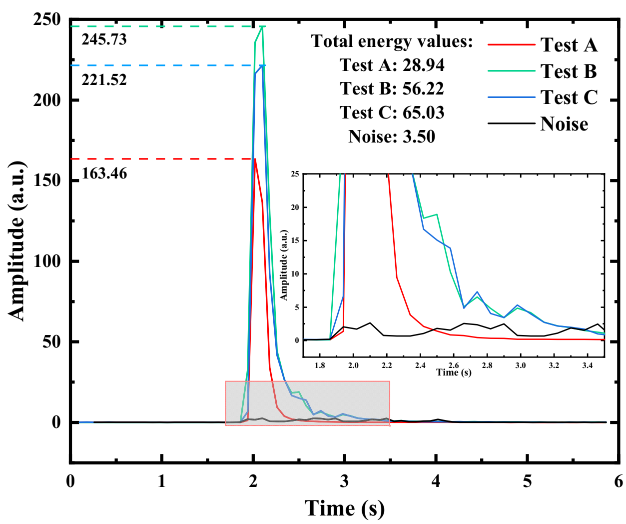

Fig. 12 Short-time energy diagram of the de-noise signal of three groups of broken wire signals and noise signals

Since the wires in the PCCP pipelines are subjected to both pre-stress and internal water pressure while conveying water, meanwhile, the vibration energy is "stored" in the water and dissipates more slowly when the pipe is full, the energy released at the time of fracture is greater and frequently lasts.

The prototype test shows that the wire breaks monitoring of PCCP based on DAS technology is feasible and capable of capturing the occurrence of wire breaks more efficiently. In practical applications, DAS may be influenced by many factors such as monitoring length, complex environment, etc. The amount of data collected is enormous, therefore, it is necessary to identify signals simply, quickly, and effectively. Wire break signals in different environments have both similarities and differences, meanwhile, wire breaks and environment noise could be identified and jointly judged from time-domain features such as signal amplitude, short-time zero-crossing rate, and short-time energy.

5 Conclusion

In this paper, a monitoring method of breaking wires in PCCP based on phase-sensitive optical time-domain reflectometry (Φ-OTDR) is proposed using Distributed Fiber Acoustic Sensing (DAS). A PCCP with an inner diameter of 3.4 m and a length of 5 m was applied in this test. The main purpose of this paper aims to identify and compare the broken wire signals at different locations in the PCCP under different environments, and distinguish them from noise. The main concluding remarks of the study are the following:

- The fiber installed at various locations in the PCCP was able to capture the occurrence of break wires instantly, and accurately, while the signals at both ends of the fiber are promiscuous.
- Wire break signals in different environments have both similarities and differences. From the time-domain perspectives of amplitude, duration, short-time zero-crossing rate, and short-time energy, the wire's break and noise can be effectively discriminated.
- As the internal water pressure rises, the energy released at fracture is larger and the signal lasts longer. The wires will break without warning after reaching the cross-sectional critical stress, which is sudden and unpredictable, and difficult to predict.
- The essence of prestressed wire breaks is the release of internal energy. The waveform of the wire break signal is proportional to the magnitude of the internal water pressure and is independent of the causing the wire breaks, such as corrosion and hydrogen embrittlement.

Distributed fiber optic acoustic sensing technology has favorable development prospects in the field of pipeline structural safety monitoring. In the next step, the operation of PCCP pipelines will be monitored for a long time, relying on a water transmission project, and the positioning of wire breaks will be studied.

Acknowledgements This research was supported by the National Science Fund for Distinguished Young Scholars (No. 52125904), Shaanxi Natural Science Basic Research Program (No. 2021JLM-46), and Program 2022TD-01 for Shaanxi Provincial Innovative Research Team (No. 2022TD-01). The authors would like to thank PowerChina Shandong Pipeline Engineering Corporation Limited for the support and help in the experiment.

References

1. Kuwairi A (2006) Water mining: the great man-made River. Libya Civil Eng 159(5):39–43. https://doi.org/10.1680/cien.2006.159.5.39
2. Huang J, Zhou Z, Zhang D (2013) A fiber Bragg grating pressure sensor and its application to pipeline leakage detection. Adv Mech Eng 2013(2):1310–1313. https://doi.org/10.1155/2013/590451
3. Semanuik SM, Mergelas B (2006) Comparison of identified distress in CCP pipelines operated by water utilities in North America. Service to the Owner, Pipelines, pp 1–8. https://doi.org/10.1061/40854(211)21
4. Ball RT, Moore WG, Smith DL (2012) Prestressed concrete cylinder pipe rehabilitation repair and replacement: large diameter success stories. Fla Water Resour J 4–10
5. Singh SK (2000) Corrosion studies on prestressing steel wires. Imperial College London. http://hdl.handle.net/10044/1/7773
6. Alvarez MG, Galvele JR (1984) The mechanism of pitting of high purity iron in NaCl solutions. Corros Sci 24(1):27–48. https://doi.org/10.1016/0010-938x(84)90133-1
7. Turnbull A, McCartney LN, Zhou S (2006) A model to predict the evolution of pitting corrosion and the pit-to-crack transition incorporating statistically distributed input parameters. Corrosion Sci 48(8):2084–2105. https://doi.org/10.1016/j.corsci.2005.08.010 (**ISSN 0010-938X**)
8. Zhai K, Fang H, Guo C et al (2020) Strengthening of PCCP with broken wires using prestressed CFRP. Constr Build Mater 267(7):120903. https://doi.org/10.1016/j.conbuildmat.2020.120903 (**ISSN 0950-0618**)
9. Zhai K, Fang H, Fu B et al (2020) Mechanical response of externally bonded CFRP on repair of PCCPs with broken wires under internal water pressure. Constr Build Mater 239:117878. https://doi.org/10.1016/j.conbuildmat.2019.117878
10. Zhai K, Fang H, Guo C et al (2021) Full-scale experiment and numerical simulation of prestressed concrete cylinder pipe with broken wires strengthened by prestressed CFRP. Tunn Undergr Space Technol. https://doi.org/10.1016/j.tust.2021.104021
11. Zhai K, Guo C, Fang H, Li B, Wang F (2021) Stress distribution and mechanical response of pccp with broken wires. Eng Struct 245(5):112858. https://doi.org/10.1016/j.engstruct.2021.112858
12. Hu BY, Fang HY, Wang FM, Zhai KJ (2019) Full-scale test and numerical simulation study on load-carrying capacity of prestressed concrete cylinder pipe (PCCP) with broken wires under internal water pressure. Eng Failure Anal 104:513–530. https://doi.org/10.1016/j.engfailanal.2019.06.049 (**ISSN 1350-6307**)
13. Wardany RA (2010) Condition assessment of prestressed concrete cylindrical water pipes. In: 60th annual WCWWA conference and trade show, pp 1–9
14. Rizzo P (2010) Water and wastewater pipe nondestructive evaluation and health monitoring: a review. Adv Civil Eng 2010:304–316. https://doi.org/10.1155/2010/818597
15. Liu Z, Kleiner Y (2013) State of the art review of inspection technologies for condition assessment of water pipes. Measurement 46(1):1–15. https://doi.org/10.1016/j.measurement.2012.05.032
16. AWWA C304-2014 (2014) Standard for design of prestressed concrete cylinder pipe. American Water Works Association: Denver, CO, USA
17. Stroebele A, Bell G, Paulson PO (2010) PCCP damage during depressurization/pressurization cycles. Pipeline division specialty conference
18. Basu S, Thirumalaiselvi A, Sasmal S, Kundu T (2021) Nonlinear ultrasonics-based technique for monitoring damage progression in reinforced concrete structures. Ultrasonics 115:106472. https://doi.org/10.1016/j.ultras.2021.106472 (**ISSN0041-624X**)
19. Lin SB, Shams S, Choi H (2018) Hoda Azari, Ultrasonic imaging of multi-layer concrete structures. NDT&E Int 98:101–109. https://doi.org/10.1016/j.ndteint.2018.04.012 (**ISSN 0963-8695**)
20. Yılmaz B, Jasiūnienė E (2020) Advanced ultrasonic NDT for weak bond detection in composite-adhesive bonded structures. Int J Adhes Adhes 102:102675. https://doi.org/10.1016/j.ijadhadh.2020.102675 (**ISSN 0143-7496**)
21. Hisham AE, Rhys P, Karen MH (2013) Damage assessment of corrosion in prestressed concrete by acoustic emission. Constr Build Mater 40:925–933. https://doi.org/10.1016/j.conbuildmat.2012.11.071 (**ISSN 0950-0618**)
22. Noorsuhada MN (2016) An overview on fatigue damage assessment of reinforced concrete structures with the aid of acoustic emission technique. Constr Build Mater 112:424–439. https://doi.org/10.1016/j.conbuildmat.2016.02.206
23. Lesage JC, Sinclair AN (2015) Characterization of prestressed concrete cylinder pipe by resonance acoustic spectroscopy. J Pipeline Syst Eng Pract 6(1):04014011. https://doi.org/10.1061/(ASCE)PS.1949-1204.0000180
24. Dérobert X, Lataste JF, Balayssac JP, Laurens S (2017) Evaluation of chloride contamination in concrete using electromagnetic non-destructive testing methods. NDT & E Int 89:19–29. https://doi.org/10.1016/j.ndteint.2017.03.006 (**ISSN 0963-8695**)
25. Xie YB, Feng H, Zhao MX, Zeng ZM (2019) PCCP broken wire detection based on orthogonal electromagnetic principle. J Measure Sci Instrum. https://doi.org/10.3969/j.issn.1674-8042.2019.01.012
26. Cheng BQ, Dou TS, Xia SF, Zhao LJ, Yang JX, Zhang Q (2020) Mechanical properties and loading response of prestressed concrete cylinder pipes under internal water pressure. Eng Struct 216:110674. https://doi.org/10.1016/j.engstruct.2020.110674 (**ISSN0141-0296**)
27. Zhu WX, Shen QX, Qin HY (2021) Monitoring of prestress and bond stress of self-sensing FBG steel strand. Measurement 177:109246. https://doi.org/10.1016/j.measurement.2021.109246 (**ISSN0263-2241**)
28. Huang J, Zhou Z, Zhang D (2013) A fiber Bragg grating pressure sensor and its application to pipeline leakage detection. Adv Mech Eng. https://doi.org/10.1155/2013/590451
29. Huang J, Zhou Z, Zhang D (2016) Online monitoring of wire breaks in prestressed concrete cylinder pipe utilising fiber Bragg grating sensors. Measurement 79:112–118. https://doi.org/10.1016/j.measurement.2015.10.033
30. Wei H, Liao K, Zhao X (2019) Low-coherent fiber-optic interferometry for in situ monitoring the corrosion-induced expansion of pre-stressed concrete cylinder pipes. Struct Health Monit 18(5–6):1862–1873. https://doi.org/10.1177/1475921719826360
31. Huang LL, Li YC, Chen S, Zhang QW, Song YX, Zhang JJ, Wang M (2020) Building safety monitoring based on extreme gradient boosting in distributed optical fiber sensing. Opt Fiber Technol 55:102149. https://doi.org/10.1016/j.yofte.2020.102149 (**ISSN 1068-5200**)
32. Cao WH, Cheng GL (2021) Modeling and experimental research on receiving signal of multi-layer distributed acoustic sensing optical fiber in shallow water. Opt Fiber Technol 67:102692. https://doi.org/10.1016/j.yofte.2021.102692 (**ISSN 1068-5200**)
33. Muggleton JM, Hunt R, Rustighi E, Lees G, Pearce A (2020) Gas pipeline leak noise measurements using optical fiber distributed acoustic sensing. J Natural Gas Sci Eng 78:103293. https://doi.org/10.1016/j.jngse.2020.103293 (**ISSN 1875-5100**)
34. SL 702-2015 (2015) Technical specifications of prestressed concrete cylinder pipe. China Water and Power Press, Beijing, China (**in Chinese**)
35. Li X, Zeng Y, Muchiri ND, Yan W, Feng Y (2022) The use of distributed acoustic sensing (DAS) in monitoring the integrity of

cement-casing system. J Petroleum Sci Eng E 208:109690. https://doi.org/10.1016/j.petrol.2021.109690 (**ISSN 0920-4105**)

36. Nikles M, Bosson R (2009) Long-distance fiber optic sensing solutions for pipeline leakage, intrusion, and ground movement detection. Proc SPIE 7316(5):731602. https://doi.org/10.1117/12.818021
37. Grandi S, Dean M, Tucker O (2017) Efficient containment monitoring with distributed acoustic sensing: feasibility studies for the former Peterhead CCS Project. Energy Proc 114:3889–3904. https://doi.org/10.1016/j.egypro.2017.03.1521 (**ISSN 1876-6102**)
38. Bandweaver CC (2015) An introduction to fibre optic intelligent distributed acoustic sensing (iDAS) technology for power industry applications. In: 9th International conference on insulated power cables
39. Alistair M, Chris M, Walter J et al (2003) Detection of hydrocarbon fuel spills using a distributed fibre optic sensor. Sens Actuators A 109(1):60–67. https://doi.org/10.1016/j.sna.2003.09.007
40. Hubbard PG et al (2021) Dynamic structural health monitoring of a model wind turbine tower using distributed acoustic sensing (DAS). J Civil Struct Health Monit 3:833–849. https://doi.org/10.1007/s13349-021-00483-y

Publisher's Note Springer Nature remains neutral with regard to jurisdictional claims in published maps and institutional affiliations.

Springer Nature or its licensor holds exclusive rights to this article under a publishing agreement with the author(s) or other rightsholder(s); author self-archiving of the accepted manuscript version of this article is solely governed by the terms of such publishing agreement and applicable law.